



Novel amphiphilic chitosan derivatives: Synthesis, characterization and micellar solubilization of rotenone

Shui-Bing Lao^a, Zhi-Xiang Zhang^a, Han-Hong Xu^{a,*}, Gang-Biao Jiang^{b,*}

^a Key Laboratory of Natural Pesticide and Chemical Biology, Ministry of Education, South China Agricultural University, Guangzhou 510642, PR China

^b Department of Pharmaceutical Engineering, College of Resource and Environment, South China Agricultural University, No. 483, Wushan Road, Guangzhou 510642, PR China

ARTICLE INFO

Article history:

Received 14 March 2010

Received in revised form 21 June 2010

Accepted 25 June 2010

Available online 4 July 2010

Keywords:

Chitosan derivatives

Rotenone

Polymer micelles

Solubilization

ABSTRACT

Novel amphiphilic chitosan derivatives N-(octadecanol-1-glycidyl ether)-O-sulfate chitosan (NOSCS) with octadecanol glycidyl ether as hydrophobic groups and sulfate as hydrophilic groups were synthesized successfully. The NOSCS were characterized with ¹H NMR, FT-IR, and their critical micellar concentrations (CMCs) were found to be 3.55×10^{-3} to 5.50×10^{-3} mg/mL. The degree of substitution (DS) of octadecanol glycidyl ether grafted on chitosan was ranging from 0.6% to 7.1%. NOSCS could form polymeric micelles with the size of 167.7–214.0 nm by self-assembly in aqueous solution. Rotenone, a water-insoluble botanical insecticide, was entrapped into NOSCS micelles solution by reverse micelle method. And the highest rotenone concentration was up to 26.0 mg/mL, which was much higher than that in water (0.002 mg/mL). Therefore, NOSCS nano micelles may be useful as a prospective carrier for control released agrochemical.

Crown Copyright © 2010 Published by Elsevier Ltd. All rights reserved.

1. Introduction

Botanical insecticides contain mixtures of biologically active substances, safer to human and environment than conventional pesticides, have been used progressively (Dayan, Cantrell, & Duke, 2009). Some of them are prepared to aqueous solutions (AS) or soluble liquid (SL), such as matrine, oxymatrine, veratridine, most of others are prepared to emulsifiable concentrate (EC) formulation, for instance, azadirachtin, celangulin, pyrethrum, rotenone, nicotine, rhodojaponin-III (Hu, Kolcke, & Chiu, 1993). The current trends in the development of pesticide formulations are increased enormously to meet the needs of environmental safety, eliminate organic solvents or to improve the activity and persistence of the active ingredient (Knowles, 2008).

Rotenone is a botanical insecticide which derived from the roots or rhizomes of the tropical legumes *Derris*, *Lonchocarpus*, and *Tephrosia*. It has been used to control aphids, trips, acari for more than 150 years (Murray, 2006). Rotenone has been allowed to use in organic crop production because of its natural origin, short persistence in the environment, safety to non-target organisms and low resistance development (Nawrot, Harmatha, & Kostoval, 1989; Xu & Huang, 2001). However, the agriculture utilization of rotenone was limited, due to its proneness to degrade or isomerize in the presence of sunlight and its lack of sufficient drug persistent period for the death of insect (Chen, Xu, Yang, & Liu, 2009). In addition, rotenone

is nearly insoluble in water (0.002 mg/mL) (Hu, Xia, Zhan, Huang, & Xu, 2006), so it had been prepared to different kinds of formulations which contained large amount of organic solvents, however those organic solvents may still pollute the environment (Pan, Tao, & Zhang, 2005).

Chitosan based polymeric micelle due to its outstanding biologic properties and functions such as biodegradability (Chellat et al., 2000), biocompatibility (Risbud & Bhonda, 2000), insecticidal and antibacterial activity, has been widely researched or applied in the fields of agriculture, medicine, pharmaceuticals, functional food in the last decade (Badawy et al., 2004; Hejazi & Amiji, 2003; Kumar, Muzzarelli, Muzzarelli, Sashiwa, & Domb, 2004; Rabea et al., 2005). However, chitosan has no amphiphilicity, cannot form micelle and load drug directly. In recent years, chitosan-based micelle system has been developed by introducing hydrophobic and/or hydrophilic groups to the chitosan backbone (Zhang et al., 2008). Amphiphilic chitosan derivatives which grafted sulfuryl as hydrophilic moieties and octyl as hydrophobic moieties had been reported (Zhang, Ping, Zhang, & Shen, 2003; Zhang et al., 2008). It could form nano micelles of core-shell structure by self-assembly in aqueous environment and solubilize paclitaxel. Tien et al. (2003) reported that the long and high degree of substitution (DS) could make the structure of chitosan derivatives stable. Yao et al. (2007) prepared series N-mPEG-N-octyl-O-sulfate chitosan derivatives; however, the DS of these derivatives was rather low (0.05–0.83%), leading to high critical micellar concentrations (CMCs 1.1×10^{-2} to 7.9×10^{-2} mg/mL). Therefore the micelles may be unstable in dilute solution (Jiang, Quan, Liao, & Wang, 2006). The same situation happened to micelles of glycol chitosan modified by 5β-cholanic acid

* Corresponding authors. Tel.: +86 20 85285127; fax: +86 20 38604926.

E-mail addresses: hxxu@scau.edu.cn (H.-H. Xu), jgb3h@163.com (G.-B. Jiang).

(DS, 1.1–8.7%, CMCs, 4.7×10^{-2} to 21.9×10^{-2} mg/mL) prepared by Kwon et al. (2003).

Alkylglycidyl ether with a long alkyl chain is very important intermediates in pharmaceutical applications (Kang, Lee, Yoon, & Yoon, 2001). However, the chitosan derivatives which grafted alkylglycidyl ether have not been reported up to now. Further more, utilizing these amphiphilic polymers micelles to entrap botanical agrochemical in preparing nano pesticide formulation has not been studied yet.

In this paper, novel amphiphilic chitosan derivatives were designed and synthesized by grafting octadecanol-1-glycidyl ether to amino groups, sulfate to hydroxyl groups. The chemical structures and physical properties of the chitosan derivatives were characterized with ^1H NMR, FT-IR. The CMC was measured by using pyrene as a hydrophobic fluorescence probe. Their sizes were examined by dynamic light scattering (DLS) and the morphologies of their aggregates were observed by transmission electron microscopy (TEM). In addition, rotenone as a model drug was chosen and used to assess the potential loading capability of novel chitosan derivatives. This study may lead to a kind of novel carriers for improving the efficacy of water-insoluble agrochemical.

2. Experimental

2.1. Materials

Chitosan (M_w 33 kDa, 92% deacetylated) was obtained from Boao Biotechnology Co. (Shanghai, China). Cetyl trimethyl ammonium bromide (CTAB) was purchased from Tianjin Fu Chen chemicals reagent factory. 1-Octadecanol was purchased from Jiangsu yonghua fine chemical Co. Ltd. (China). All commercially available solvents and reagents were used without further purification.

2.2. Methods

2.2.1. Synthesis of N-(octadecanol-1-glycidyl ether)-O-sulfate chitosan derivatives (NOSCS)

2.2.1.1. Synthesis of 2-(octadecyloxymethyl)oxirane. Synthesis of 2-(octadecyloxymethyl)oxirane synthesized of OGE was improved from the method of Kang et al. (2001) as shown in Scheme 1. Toluene (30 mL) as solvent, CTAB (1.0 g) as catalyst, 1-octadecanol (0.1 M) mixed with NaOH (6.0 g) were all added to a flask (100 mL)

and melt completely by heating. After that epichlorohydrin (0.2 M) was dropped slowly into the mixture under magnetic stirring at 62°C for 2 h in the oil bath. Then stop reaction and left to cool at room temperature. The precipitate was filtrated and washed with toluene five times. The filtrate was collected and washed with 70°C water three times, and then stratified stationarily. The upper layer was collected and dried with anhydrous sodium sulfate. Toluene and CTAB were removed by steaming in the oil bath at 110°C in vacuum for half an hour. Then left to cool over night at room temperature, and the pale yellow solid was obtained.

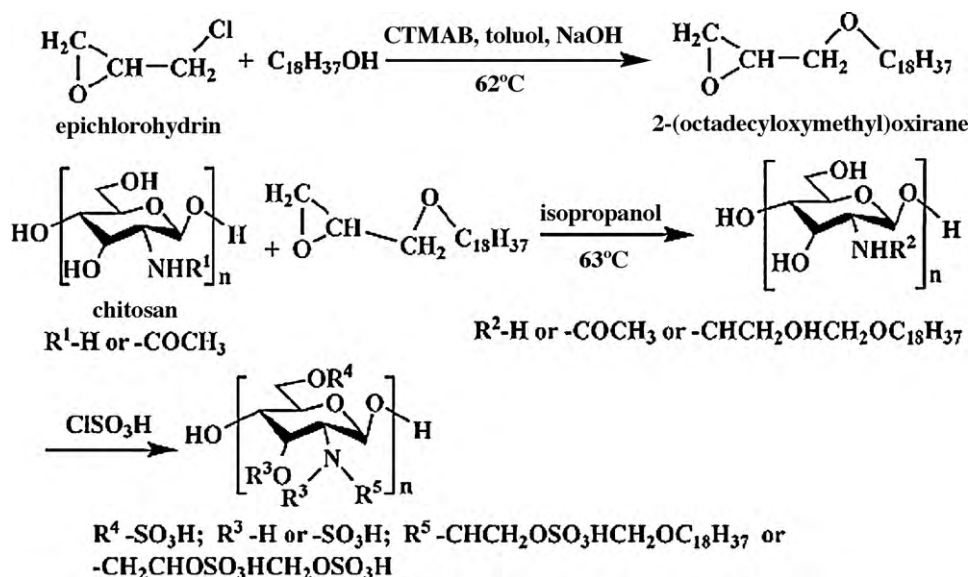
2.2.1.2. Synthesis of N-(octadecanol-1-glycidyl ether) chitosan (OGECS). The OGECS was prepared as follows: Chitosan (6.0 g) was dissolved in 120 mL of acetic acid (0.1 M), and then precipitated with 55 mL NaOH (2.0 M). The precipitate was collected by filtration and washed with distilled water to adjust the pH value of 7.0. After that incompact or swollen chitosan powder was obtained and dispersed in 70 mL of isopropanol under magnetic stirring, then certain amount of OGE (12.0 g) was added to above mixed solution and allowed to react at 63°C for 3 h. Consequently, the pure OGECS was collected by filtrating and washing with toluene five times. After drying at 60°C in vacuum for more than 6 h, the light yellow powder was obtained.

2.2.1.3. Synthesis of NOSCS. Chlorosulfonic acid (5.0–8.0 mL) was dropped slowly into formamide (40.0 mL) under magnetic stirring at 0°C . Then, OGECS (2.0 g) was added and allowed to react at 68°C for 6 h. The reaction solution was left to cool at room temperature and neutralized with aqueous 20% NaOH solution. The precipitate was collected by pouring double volumes of acetone into the mixed solution, followed by filtrating and washing with anhydrous alcohol five times. After drying at 60°C in vacuum for more than 6 h the white powder was obtained.

2.2.2. Characterization and identification

^1H NMR spectra were performed on a Bruker AV-600 MHz spectrometer. Chitosan and OGECS were dissolved in a mixed solvent of 5% CD_3COOD and D_2O , NOSCS was dissolved in D_2O and Rotenone-loaded NOSCS was dissolved in D_2O and $\text{DMSO}-d_6$ (1:1) mixed with 5% CD_3COOD .

FT-IR spectra were recorded on Fourier-transform infrared spectrometer (Nicolet Avatar 360, USA) in KBr discs.



Scheme 1. Synthesis of N-(octadecanol-1-glycidyl ether)-O-sulfate chitosan (NOSCS).

Particle size and zeta potential were performed on Zetasizer Nano ZS (Malvern, UK). A suitable amount of sample was dissolved in distilled water ultrasonic treatment for 8 min (KH-500 Ultrasonic Cleaner, China) and the size and zeta potential were measured by Dynamic light scattering (DLS).

The morphology and size distribution were observed by FEI-Tecna 12 Transmission electron microscopy (Philips Company, Holland). The Sample solution was dropped onto the carbon-coated 300 mesh copper grid and air-dried, followed by the application of methylamine tungstate negative staining for 2 min.

2.2.3. Measurement of CMC

The CMC of the NOSCS was measured by using pyrene (Sigma–Aldrich, >98%) as a hydrophobic probe in fluorescence spectroscopy (Hitachi F-4500, Japan) (Seow, Xue, & Yang, 2007; Sui, Wang, Dong, & Chen, 2008; Yao, Zhang, Ping, & Yu, 2007). Briefly, a known amount of pyrene in tetrahydrofuran was added to each of a series of 10 mL vials and the tetrahydrofuran was evaporated at room temperature, a serial amount of various concentrations of NOSCS solutions (2.56×10^{-6} to 1.0 mg/mL) were added to the vials (the final concentration of pyrene was controlled to 6.0×10^{-7} M), and then sonicated for 30 min at 28 °C. The sample solutions were heated at 40 °C for 3 h to equilibrate pyrene and the micelles, and then left to cool overnight at room temperature. Fluorescence excitation spectra were measured at the excitation wavelength (λ_{ex}) of 335 nm. Both excitation and emission bandwidths were set at 2.5 nm and the spectra were accumulated with an integration time of 240 nm/min, emission wavelength was 350–450 nm for emission spectra.

2.2.4. Preparation of rotenone-loaded nano micellar

Rotenone-loaded NOSCS micelles solution were prepared by reverse micelle method which was improved from the method described as Jiang et al. (2006). Rotenone (50 mg) was dissolved in 5–10 mL mixture of acetone and ethanol (1:1 v/v), and then NOSCS (200 mg) was added into the solution. After that, distilled water (50 mL) was dropped slowly (nearly one drop per second) into the above solution under magnetic stirring at room temperature. In this process certain portion of aggregated rotenone would be entrapped into the hydrophobic cores of NOSCS micelles. After 4 h of continuous stirring to evaporate the organic solvent, the mixed solution was lyophilized by a freeze dryer system (Sihuan lyophilizer, China). The lyophilized powder was collected and washed with acetone four times. Consequently, the rotenone outside the micelle (including the surface conglutinated and not entrapped) was collected, determined by HPLC after dilution. While the left powder was dried and preserved in –4 °C for further investigation.

2.2.5. Measurement of rotenone content in chitosan derivative micellar

The content of rotenone in the micellar was determined by HPLC (HP1100, Agilent Technologies, USA). The mobile phase was a mixture of acetonitrile and water (80:20, v/v). The column was a Diamohsile™ C₁₈ (250 mm × 4.6 mm, 10 μm). The flow rate was 1.0 mL/min, the detection wavelength was 299 nm, the column temperature was 28 °C, injected volume of the sample was 10 mL.

The drug loading capacity (LC) and encapsulation efficiency (EE) of NOSCS were calculated by using the following equations respectively (Gupta and Ravkumar, 2001).

$$LC = \frac{A - B}{C} \quad (1)$$

$$EE = \frac{A - B}{A} \quad (2)$$

where A total amount of added Rotenone; B free amount of Rotenone; C weight of NOSCS.

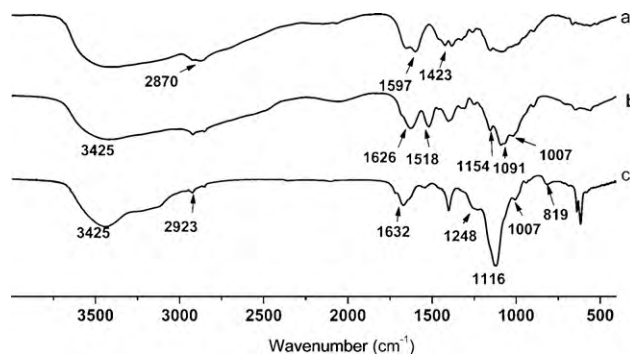


Fig. 1. FT-IR spectra of (a) chitosan, (b) OGECS and (c) NOSCS.

2.2.6. In vitro drug release studies of rotenone-loaded NOSCS

Lyophilized micelles powder (5 mg) containing known rotenone or rotenone solution mixed in NOSCS-3 powder were dissolved in 2 mL of phosphate buffer solution (PBS) (0.1 M, pH 9.0 and containing 20% ethanol). The resulting solution was placed into dialysis bags (cutoff molecular weight: 14,000), and then the dialysis bags were introduced into vial containing 80 mL of PBS (the same as the solution added in the dialysis bag). The systems were immersed in a thermostatic bath with a speed of 100 rpm at 23 °C (average temperature of Guangdong province). At appropriate intervals, 2 mL samples of solution were withdrawn from the vials and replaced by 2 mL of fresh PBS. The drug release was assayed by UV spectrophotometer at 299 nm.

3. Results and discussions

3.1. Synthesis and characterization of chitosan derivatives

The synthetic route of NOSCS was briefly summarized in Scheme 1. Structures change of chitosan derivatives were confirmed by FT-IR spectra (Fig. 1), ¹H NMR spectra (Fig. 2). The N–H stretching and O–H stretching vibrations can be characterized by the broad peak in the region of 3200–3500 cm^{–1} (Fig. 1a–c). Chitosan showed a distinct primary amino groups bending vibration at 1597 cm^{–1}, while the amine group of chitosan was grafted, the absorption peak of 1597 cm^{–1} almost disappeared, prominent bands at 1626 and 1518 cm^{–1} were observed (Fig. 1b). The peaks at 1154 and 1091 cm^{–1} from 3 –OH and 6 –OH of chitosan almost disappeared, and the new peaks at 1248, 1116 and 819 cm^{–1} were assigned to the O=S=O bonds of N-sulfate groups (Yao et al., 2007). These results indicated that sulfate groups were introduced into 3 –OH and 6 –OH groups of OGECS. The peaks at 1007 cm^{–1} was assigned to the asymmetric extension vibration of C–O–C bonds of chitosan derivative.

The ¹H NMR assignments of OGECS (Fig. 2b) were characterized as follows: ¹H NMR (D₂O) δ 3.05 ppm (H-2), δ 3.34–3.80 ppm to the ring protons (H-3, 4, 5, 6), δ 1.92 ppm methene hydrogen (–NHCOCH₃). Compared with chitosan (a), the ¹H NMR spectrum of the OGECS and NOSCS were shown that the signals at δ 3.2 ppm were assigned to the methenyl hydrogen (–NHCHCH₂OHCH₂OC₁₈H₃₇) of the N-alkyl group. The signals at δ 1.1–1.4 ppm were assigned to the methene hydrogen (–NHCHCH₂OH –CH₂OCH₂ (CH₂)₁₆CH₃), the peaks δ 0.71 ppm (c), δ 0.73 ppm (b), were attributed to the methyl hydrogen –NHCHCH₂OHCH₂OCH₂ (CH₂)₁₆CH₃.

The ¹H NMR spectrum of rotenone-loaded NOSCS in D₂O was similar to that of the derivative itself as presented in Fig. 2c, which revealed that rotenone was utterly encapsulated by the NOSCS, and NOSCS can self-aggregate in D₂O to some extent; however, after ultrasonic treatment at 50 °C for 30 min, the rotenone carbonyl signals at δ 1.70, δ 6.50–6.60, δ 7.70 emerged (Fig. 3c), which

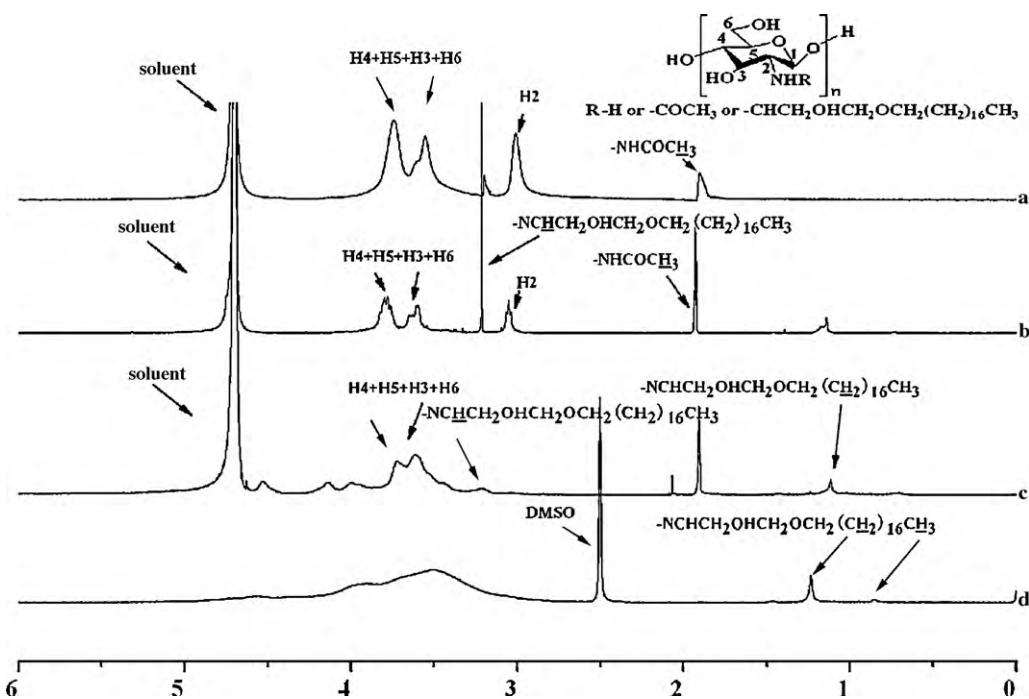


Fig. 2. ^1H NMR spectra of (a) chitosan and (b) OGECS in D_2O mixed with 5% CD_3COOD , (c) NOSCS in D_2O and (d) NOSCS in $\text{DMSO}-d_6$.

revealed that the rotenone was released from the polymer micelles after being ultrasonic treatment in D_2O and DMSO mixed with 5% CD_3COOD in 50°C .

The DS defined as the number of OGE groups per 100 sugar residues of chitosan, was calculated by ^1H NMR using the ratio of NOSCS methyl protons peak area (δ 0.73 ppm) to three times H-2 protons peak area (δ 3.02 ppm) of glucosamine ring (Ma, Yang, Kennedy, & Nie, 2009; Yang et al., 2008). Three different amount of OGE were grafted on chitosan and the DS were in range of 0.6–7.1 as shown in Table 1. According to the results of ^1H NMR, FT-IR, the suggested chemical structure of NOSCS was confirmed.

As its rigid crystalline structure, poor process ability, chitosan had been limited to be utilized widely. In order to resolve these problems, chemical modification of chitosan by N-alkylation (Liu et al., 2003), N,O-acylation (Zong, Kimura, Takahashi, & Yamane, 2000), N-acylation (Jiang et al., 2006) had been studies. The alkyl bromide and acyl chloride were so active that, nearly both amino and amide groups of the original chitosan were imided. Jiang et

al. (2006) modified chitosan with palmitic anhydride and justified that palmitic acyl group was just covalently linked amino group of chitosan. Form the result we could speculate that at certain situation amino group of chitosan was more active than hydroxy. OGE was introduced to the amino group of chitosan, and the maximum DS could up to 7.1, which was a little high than Donges, Soden, Reichel, and Darmstadt (2000) reported 1.5 to 2.0, maybe we used pure solvent rather than mixed solvent. Chlorosulfonic acid was so active that it could imide the rest amino and hydroxy group of chitosan and became hydrophilic sulfonyl group.

3.2. Characteristics of NOSCS self-assembled nano micelles

Based on the experiment observations, when NOSCS dissolved in water they could form self-assembled micelles with the sizes from 167.7 to 214.0 nm and zeta potential from -45.0 to -51.9 mV as shown in Table 1. The particle sizes decreased as the DS increased, which might indicate that more hydrophobic substitution resulted in more compact and stable micelles. This phenomenon was consistent with the results reported by Lee et al. (1998) and Kwon et al. (2003). The particle size of NOSCS-2 and NOSCS-3 with the DS of 1.0 and 7.1 were significantly smaller than that of NOSCS-1. The increase of DS could enhance the chances of hydrophobic interactions among hydrophobic pendant groups, resulting in the formation of more compact hydrophobic cores (Jiang et al., 2006). The TEM observation was shown in Fig. 4a. It was depicted that the shapes of NOSCS-3 were approximately spherical,

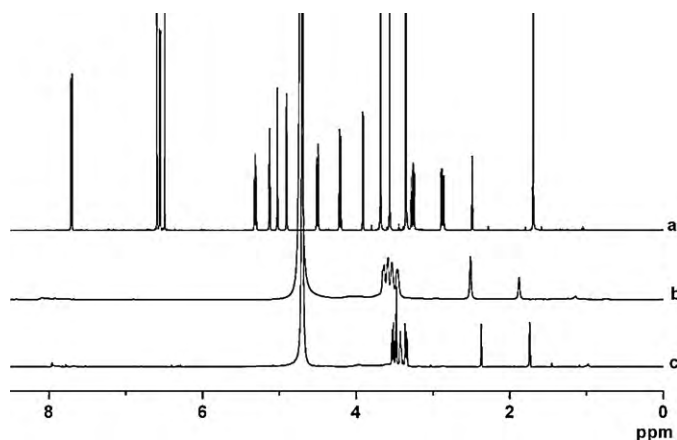


Fig. 3. ^1H NMR spectra of (a) Rotenone in $\text{DMSO}-d_6$, (b) Rotenone-loaded NOSCS in D_2O and (c) Rotenone-loaded NOSCS in D_2O and $\text{DMSO}-d_6$ (1:1) mixed with 5% CD_3COOD in 50°C after being ultrasonic treatment for 30 min.

Table 1
Characteristics of NOSCS self-assembled nano micelles.

Sample	DS ^a (%)	size ^b (nm)	Zeta potential (mV)	CMC (mg/mL)
NOSCS-1	0.6	$214.0 \pm 4.6a$	-51.9 ± 0.5	5.50×10^{-3}
NOSCS-2	1.0	$180.7 \pm 3.8b$	-45.0 ± 0.4	5.24×10^{-3}
NOSCS-3	7.1	$167.7 \pm 10.7b$	-46.2 ± 2.6	3.55×10^{-3}

^a The data in the table were "Mean \pm SE", values followed by different letters were significantly different according to Duncan's multiple range test ($P < 0.05$).

^b DSs determined from the integration resonance ratio of the CH_3 groups within OGE blocks vs H-2 of chitosan residues detected by ^1H NMR.

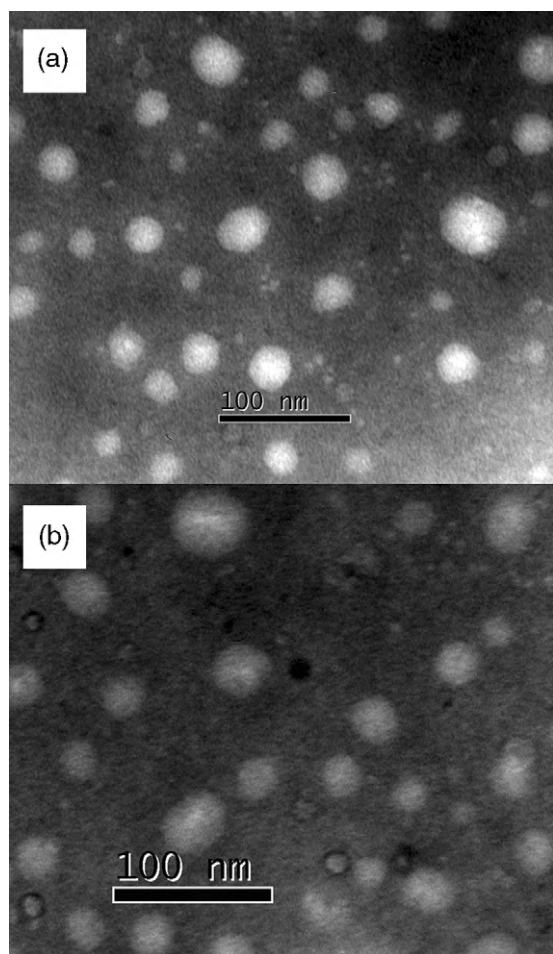


Fig. 4. TEM micrograph of NOSCS (a) and Rotenone-loaded NOSCS nano micelles (b).

and the sizes observed were less than 100 nm. However, the sizes were much smaller than the results measured by DLS (Table 1), and this may be ascribed to the different state of aggregates. Because the samples were dried and the aggregates shrank in the process of TEM observations, while the samples measured by DLS were in aqueous solution (Wang, Liu, Weng, & Zhang, 2007).

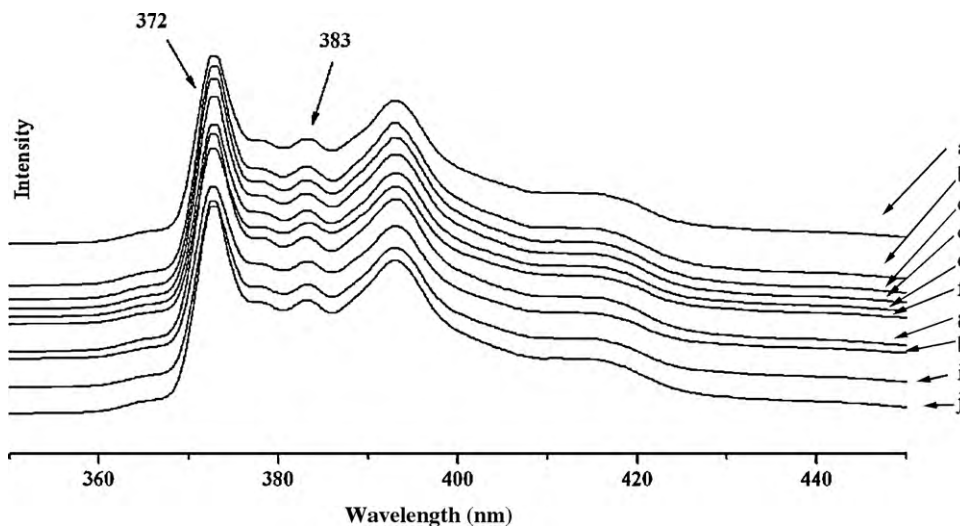


Fig. 5. Emission spectra of pyrene (6.0×10^{-7} mg/mL) as a function of NOSCS-3 concentration: (a) 1, (b) 0.5, (c) 0.2, (d) 0.04, (e) 0.008, (f) 0.0016, (g) 0.00032, (h) 0.000064, (i) 0.000012, and (j) 0.00000256 mg/mL in water.

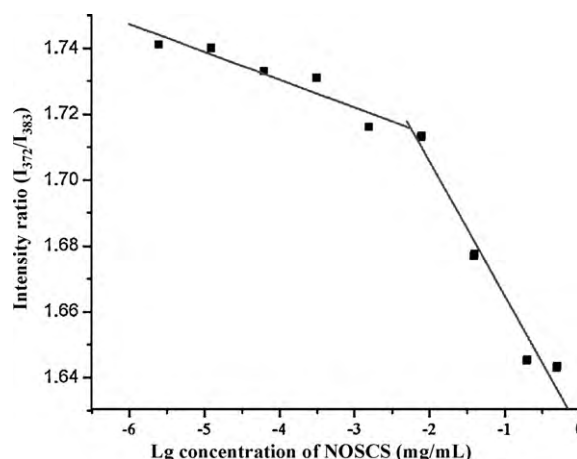


Fig. 6. Change of intensity ratio (I_{372}/I_{383}) for pyrene in water with various concentrations of NOSCS-3.

3.3. Measurement of CMC

Fig. 5 showed that the fluorescence emission spectra of pyrene incorporated into self-aggregates of NOSCS-3 in water at 25 °C. The total emission intensity increased while the concentration of NOSCS in dilute aqueous solution increased. The same situation was also reported by Jiang et al. (2006). There were five peaks in the emission spectra of pyrene, and the emission intensity ratio of the first peak (372 nm, I_1) and the third peak (383 nm, I_3) had been used to monitor the aggregation behavior of surfactants or polymers in polar solution (Amiji, 1995; Jiang et al., 2006). The CMC was calculated by the crossover point as Yao et al. (2007) described. The changes of the intensity ratio of I_1/I_3 vs logarithm of the polymer concentration were shown in Fig. 6. A linear decrease was observed when the polymeric concentration was above CMC. The CMCs values of NOSCS-3, NOSCS-2 and NOSCS-1 were from 3.55×10^{-3} to 5.50×10^{-3} mg/mL shown in Table 1. They were lower than that of Yao et al. (2007), who synthesized a series of N-mPEG-N-octyl-O-sulfate chitosan derivatives with the CMCs from 0.011 to 0.079 mg/mL. It could be noticed that the CMC values decreased with increasing DS. This phenomenon is consistent with the results reported by Li and Kwon (2000).

Table 2

Characteristics of Rotenone-loaded NOSCS self-assembled nano micelles.

Sample	Rotenone-loading capacity (%)	Encapsulation efficiency (%)	Particle size ^a (nm)	Rotenone concentration (mg/mL)
NOSCS-1	11.68	5.90	216.0 ± 2.1a	26.0
NOSCS-2	21.63	4.95	116.4 ± 0.3c	20.6
NOSCS-3	31.44	9.15	151.7 ± 1.1b	21.5

^a The data in the table were "Mean ± SE", values followed by different letter are significantly different according to Duncan's multiple range test ($P < 0.05$).

3.4. Characterization of rotenone-loading chitosan derivative micelles

The characterization of rotenone-loading capacity, encapsulation efficiency and particle size of rotenone-loaded micelles of chitosan derivative were listed in Table 2. It was showed that NOSCS-3 with the DS (7.1) had the highest rotenone-loading capacity (31.44%) and encapsulation efficiency (9.15%). Probably as the DS increased more OGE groups formed the hydrophobic core of the micelles which increased the rotenone-loading capacity. The particle size of rotenone-loaded NOSCS-2 and NOSCS-3 were 116.4 and 151.7 nm, which were smaller than that of rotenone-unloaded polymer micelles. Probably there had been the hydrophobic interaction between chitosan derivative and rotenone. The particle size of NOSCS-1 loading rotenone was the same as unloaded-rotenone, that maybe in the low DS of NOSCS micelles core, the hydrophobic interaction between NOSCS and rotenone was faint and the size effect was not obvious. The highest concentration of rotenone (entrapped in NOSCS) in aqueous solution were in the range of 20.6–26.0 mg/mL as showed in Table 2. Moreover, the rotenone concentration in NOSCS-1 was up to 26.0 mg/mL, which was about 13000 times higher than that of free rotenone in water (0.002 mg/mL).

Morphology of rotenone-loaded NOSCS micelles was observed by TEM. It was seen that the rotenone-loaded NOSCS (Fig. 4b) was approximately spherical. The size was all smaller than of 100 nm, and the values were obviously smaller than the data determined by DLS (Table 2).

3.5. In vitro release of rotenone-loaded NOSCS micelles

The drug release behavior of rotenone-loaded NOSCS micelles was evaluated in vitro. Compared with rotenone solution, NOSCS micelles showed a good drug control released capacity, it took about 150 h to release 70% of the drug loaded, and took more than 230 h to reach the maximum release (Fig. 7). In comparison, 70% of

rotenone released from dialysis bags within 9 h and the release was almost completely after 27 h. There was an obvious burst released effect between 110 and 150 h and then slowed down. One possible explanation for this phenomena was that some significant dissociation of the micelles had happened and the structure of micelles become loose. While the rest of the rotenone loaded in micelle structure did not collapse completely, it released slowly in the final phase. The reason was probably that the increase of rotenone concentration in the medium effected its diffusion, further more some interactions between rotenone and NOSCS probably existed, such as the hydrophobic attraction between rotenone and octadecanol-1-glycidyl ether groups and hydrogen bond interaction between the carbonyl group of rotenone and the amino group and hydroxyl group of NOSCS; all of these interactions could retard the drug sustained-release.

4. Conclusions

Novel chitosan derivatives N-3-(octadecanol-1-glycidyl ether)-O-sulfate, which formed micelles with particle sizes of 167.7–214.0 nm and zeta potential of −45.0 to −51.9 mV, had been synthesized successfully. The chemical and physical properties of NOSCS were characterized by ¹H NMR, FT-IR. NOSCS can self-assembly of approximately spherical morphology in distilled water and the CMCs were found to be 3.55×10^{-3} to 5.50×10^{-3} mg/mL. The insecticide rotenone was loaded and formed about 116.4–216.0 nm nanoparticles, and its solubility in NOSCS micelles aqueous solution was increased largely. The highest concentration of rotenone was up to 26.0 mg/mL (NOSCS-1), which was about 13000 times that of free rotenone in water (about 0.002 mg/mL). The NOSCS as a novel carrier will be further used to encapsulate and control released water-insoluble natural agrochemical to apply in organic agriculture.

Acknowledgments

The authors thank the financial support provided by the Natural Science Foundation of China (20874032), Guangdong province key project on agriculture field (2009A020101003), Science and Technology Planning Project of Guangdong Province, China (2008B0301202). Doctor Zhijun Song is gratefully acknowledged for recording the NMR spectra.

References

- Amiji, M. M. (1995). Pyrene fluorescence study of chitosan self-association in aqueous solution. *Carbohydrate Polymers*, 26, 211–213.
- Badawy, M. E. I., Rabea, E. I., Rogge, T. M., Stevens, C. V., Smagghe, G., et al. (2004). Synthesis and fungicidal activity of new N,O-acyl chitosan derivatives. *Biomacromolecules*, 5, 589–595.
- Chellat, F., Tabrizian, M., Dumitriu, S., Chornet, E., Rivard, C. H., & Yahia, L. H. (2000). Study of biodegradation behavior of chitosan-xanthan microspheres in simulated physiological media. *Journal of Biomedical Materials Research*, 53, 592–599.
- Chen, X. J., Xu, H. H., Yang, W., & Liu, S. Z. (2009). Research on the effect of photoprotectants on photostabilization of rotenone. *Journal of Photochemistry and Photobiology B: Biology*, 95, 93–100.
- Dayan, F. E., Cantrell, C. C., & Duke, S. O. (2009). Natural products in crop protection. *Bioorganic & Medicinal Chemistry*, doi:10.1016/j.bmc.2009.01.046
- Donges, R., Soden, B., Reichel, D., Darmstadt, et al. (2000). Process for the preparation and work-up of N-hydroxyalkylchitosan soluble in aqueous medium. *U.S. Patent* 6,090,928.

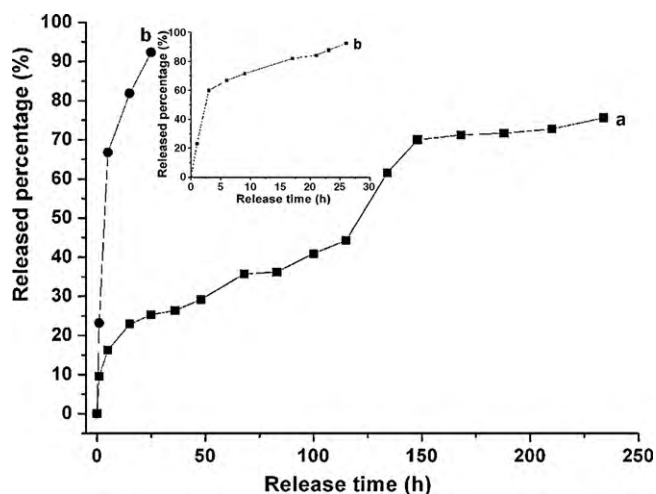


Fig. 7. In vitro release of rotenone from (a) rotenone-loaded NOSCS7.1 micelle, (b) rotenone solution mixed in NOSCS7.1 powder in PBS (0.1 M, pH 9.0), at 23 °C ($n = 3$).

- Gupta, K. C., & Ravkumar, M. N. V. J. (2001). pH dependent hydrolysis and drug release behavior of chitosan/poly (ethylene glycol) polymer network microspheres. *Journal of Material Science: Materials in Medicine*, 12, 753–759.
- Hejazi, R., & Amiji, M. (2003). Chitosan-based gastrointestinal delivery systems. *Journal of Controlled Release*, 89, 151–165.
- Hu, M. Y., Kolcke, J. A., & Chiu, S. F. (1993). Response of five insects to botanical insecticides, rhodojaponin-III. *Journal of Economic Entomology*, 86(3), 706–711.
- Hu, L., Xia, J., Zhan, S. L., Huang, X. D., & Xu, H. H. (2006). The preparation and characterizations of rotenone cyclodextrin inclusion complex the bioactivity against *Bursaphelenchus Xylophilus*. *Journal of East China Jiaotong University*, 23(1), 164–168.
- Jiang, G. B., Liao, K. R., Quan, D. P., & Wang, H. H. (2006). Novel polymer micelles prepared from chitosan grafted hydrophobic groups for drug delivery. *Molecular Pharmaceutics*, 3(2), 152–160.
- Kang, H. C., Lee, B. M., Yoon, J., & Yoon, M. (2001). Improvement of the phase-transfer catalysis method for synthesis of glycidyl ether. *Journal of the American Oil Chemists Society*, 78(4), 423–429.
- Knowles, A. (2008). Recent developments of safer formulations of agrochemicals. *Environmentalist*, 28, 35–44.
- Kumar, M. N. V. R., Muzzarelli, R. A., Muzzarelli, C., Sashiwa, H., & Domb, A. J. (2004). Chitosan chemistry and pharmaceutical perspectives. *Chemical Reviews*, 104, 6017–6084.
- Kwon, S. K., Park, J. H., Chung, H., Kwon, I. C., & Jeong, S. Y. (2003). Physicochemical characteristic of self-assembled nanoparticles based on glycol chitosan bearing 5 β -cholanic acid. *Langmuir*, 19, 10188–10193.
- Lee, K. Y., Jo, W. H., Kwon, I. C., Kim, Y. H., & Jeong, S. Y. (1998). Physicochemical characteristics of self-aggregates of hydrophobically modified chitosan. *Langmuir*, 14, 3239–3233.
- Li, Y., & Kwon, G. S. (2000). Methotrexate esters of poly (ethylene oxide)-block-poly (2-hydroxyethyl-L-aspartamide) Part 1: Effects of the level of Methotrexate conjugation on the stability of micelles and drug release. *Pharmaceutical Research*, 17, 607–611.
- Liu, W. G., Zhang, X., Sun, S. J., Sun, G. J., Yao, K. D., et al. (2003). N-alkylated chitosan as a potential nonviral vector for gene transfection. *Bioconjugate Chemistry*, 14(4), 782–789.
- Ma, G. P., Yang, D. Z., Kennedy, J., & Nie, J. (2009). Synthesize and characterization of organic-soluble acylated chitosan. *Carbohydrate Polymers*, 75, 390–394.
- Murray, B. I. (2006). Botanical insecticides, deterrents, and repellents in modern agriculture and an increasingly regulated world. *Annual Reviews Entomology*, 51, 45–66.
- Nawrot, J., Harmatha, J., & Kostova, I. (1989). Antifeeding activity of rotenone and some derivatives towards selected insect storage pests. *Biochemical Systematics and Ecology*, 17, 55–57.
- Pan, L. G., Tao, L. M., & Zhang, X. (2005). Advances in pesticide formulation of suspension concentrate. *Plant Protection*, 17(2), 17–20.
- Rabea, E. I., Badawy, M. E. I., Rogge, T. M., Stevens, C. V., Smagghe, G., et al. (2005). Insecticidal and fungicidal activity of new synthesized chitosan derivatives. *Pest Management Science*, 61, 951–960.
- Risbud, M. V., & Bhonda, R. R. (2000). Polyacrylamide-chitosan hydrogels: In vitro biocompatibility and sustained antibiotic release studies. *Drug Delivery*, 7, 69–75.
- Seow, W. Y., Xue, J. M., & Yang, Y. Y. (2007). Targeted and intracellular delivery of paclitaxel using multi-functional polymeric micelles. *Biomaterials*, 28, 1730–1740.
- Sui, W. P., Wang, Y. H., Dong, S., & Chen, Y. J. (2008). Preparation and properties of an amphiphilic derivative of succinyl-chitosan. *Colloid and Surfaces A: Physicochemical and Engineering Aspects*, 316, 171–175.
- Tien, C. L., Lacroix, M., Szabo, P. I., & Mateescu, M. A. (2003). N-acylated chitosan: Hydrophobic matrices for controlled drug release. *Journal of Controlled Release*, 93, 1–13.
- Wang, Y. S., Liu, L. R., Weng, J., & Zhang, Q. Q. (2007). Preparation and characterization of self-aggregated nanoparticles of cholesterol-modified O-carboxymethyl chitosan conjugates. *Carbohydrate Polymers*, 69(3), 597–606.
- Xu, H. H., & Huang, J. G. (2001). Advances in the research of rotenone. *Journal of Southwest Agricultural University*, 23, 140–143.
- Yang, X. D., Zhang, Q. Q., Wang, Y. S., Chen, H., Zhang, H. Z., Gao, F. P., et al. (2008). Self-aggregated nanoparticles from methoxy poly (ethylene glycol)-modified chitosan: Synthesis; characterization; aggregation and methotrexate release in vitro. *Colloids and surfaces. B: Biointerfaces*, 61, 125–131.
- Yao, Z., Zhang, C., Ping, Q. N., & Yu, L. I. (2007). A series of novel chitosan derivatives: Synthesis, characterization and micellar solubilization of paclitaxel. *Carbohydrate Polymers*, 68, 781–792.
- Zhang, C., Ping, Q. N., Zhang, H., & Shen, J. (2003). Preparation of N-alkyl-O-sulfate chitosan derivatives and micellar solubilization of taxol. *Carbohydrate Polymers*, 54(2), 137–141.
- Zhang, C., Qu, G. W., Sun, Y. J., Wu, X. L., Yao, Z., Guo, Q. L., et al. (2008). Pharmacokinetics, biodistribution, efficacy and safety of N-octyl-O-sulphate chitosan micelles loaded with paclitaxel. *Biomaterials*, 29, 1233–1241.
- Zong, Z., Kimura, Y., Takahashi, M., & Yamane, H. (2000). Characterization of chemical and solid state structures of acylated chitosan. *Polymer*, 41, 899–906.